A&A 545, A24 (2012)
DOI: 10.1051/0004-6361/201219265


Astronomy & Astrophysics

# The $^{12}C_2/^{12}C^{13}C$ isotopic ratio in comets C/2001 Q4 (NEAT) and C/2002 T7 (LINEAR)⋆

P. Rousselot[1], E. Jehin[2], J. Manfroid[2], and D. Hutsemékers[2]

[1] University of Franche-Comté, Observatoire des Sciences de l'Univers THETA, Institut UTINAM - UMR CNRS 6213, BP 1615, 25010 Besançon Cedex, France
e-mail: rousselot@obs-besancon.fr
[2] F.R.S.-FNRS, Institut d'Astrophysique et de Géophysique, Université de Liège, Allée du 6 août 17, 4000 Liège, Belgium

Received 22 March 2012 / Accepted 5 July 2012

**ABSTRACT**

*Context.* Measuring the carbon isotope abundance ratio in comets allows one to constrain the conditions in the outer protosolar nebula. Different measurements of the $^{12}C/^{13}C$ ratio, using various molecules, have already been published for different solar system objects, such as the Sun, the Earth, the Moon, asteroids, planets, or comets. So far, all these measurements are consistent with $^{12}C/^{13}C \sim 90$, but significant differences have been observed. This ratio is remarkably constant in comets (91.0 ± 3.6) for studies based on the CN radical, but it presents stronger variations in studies based on other radicals.

*Aims.* This paper aims at measuring the $^{12}C/^{13}C$ ratio in two bright Oort cloud comets using the $^{12}C_2$ and $^{12}C^{13}C$ emission lines and an improved method. The ratios will be compared to those obtained for the same comets with another radical, CN.

*Methods.* We used the (2, 1) and (1, 0) bandheads of the $^{12}C^{13}C$, near 4723 and 4745 Å to measure the $^{12}C/^{13}C$ ratio and compared their intensity to the $^{12}C_2$ lines of the same bands. We developed a model for interpreting observational data obtained at high resolution (~70 000) using the 8.2-m Kueyen telescope (UT2) of the Very Large Telescope (VLT) with the Ultraviolet and Visual Echelle Spectrograph (UVES) in two comets: C/2001 Q4 (NEAT) and C/2002 T7 (LINEAR).

*Results.* Our modeling has provided $^{12}C/^{13}C = 85 \pm 20$ for C/2002 T7 (LINEAR) and 80 ± 20 for C/2001 Q4 (NEAT). These values are compatible with previous measurements performed with the CN radical.

**Key words.** line: identification – comets: general – comets: individual: C/2001 Q4 (NEAT) – comets: individual: C/2002 T7 (LINEAR)

## 1. Introduction

The analysis of comet composition represents a powerful tool for understanding the pristine composition of the solar system and the origin of comets. In this context it is very important to determine the isotopic ratios. So far, these ratios have been published for H, C, N, O, and S (e.g. Jehin et al. 2009, and references therein), but much work still remains to be done, both for measuring accurately their values and for studying how they can vary from molecule to molecule according to the type of comet.

The first $^{12}C/^{13}C$ ratio determinations were obtained from the $^{12}C^{13}C$ (1,0) Swan bandhead at 4745 Å for four bright comets: Ikeya 1963 I (Stawikowski & Greenstein 1964), Tago-Sato-Kosaka 1969 IX (Owen 1973), Kohoutek 1973 XII (Danks et al. 1974), and Kobayashi-Berger-Milon 1975 IX (unpublished data from Lambert and Danks mentioned by Lambert & Danks 1983; Vanysek 1977; Wyckoff et al. 2000). This bandhead is clearly separated from its $^{12}C_2$ equivalent but is strongly blended with $NH_2$ emission lines. For this reason the CN B-X (0,0) band was later favored for measuring the $^{12}C/^{13}C$ ratio. It has been used for the first time for comet 1P/Halley (Wyckoff & Wehinger 1988; Wyckoff et al. 1989; Kleine et al. 1995). Since then the CN B-X (0,0) band has been used with success for measuring the $^{12}C/^{13}C$ ratio in many comets of different origins (Manfroid et al. 2009).

Some other determinations of the $^{12}C/^{13}C$ ratio have been performed with radio spectroscopy of $H^{13}CN$. These measurements have been performed for the comets C/1995 O1 (Hale-Bopp) (Jewitt et al. 1997; Ziurys et al. 1999; Bockelée-Morvan et al. 2008) and 17P/Holmes (Bockelée-Morvan et al. 2008). All these determinations are compatible with, or close to – within the errorbars – the terrestrial ratio $^{12}C/^{13}C = 89$. Some in situ measurements have also been made thanks to the dust sample collected by the Stardust spacecraft (McKeegan et al. 2006; Stadermann et al. 2008).

In this paper we develop a new model for measuring this isotopic ratio using the (2,1) bandhead of $^{12}C^{13}C$ at 4723 Å in between the $^{12}C_2$ emission lines, as well as the (1,0) bandhead of $^{12}C^{13}C$ at 4745 Å. This model allows us to provide a determination of the $^{12}C/^{13}C$ ratio independent of the one inferred using the CN B-X (0,0) band. We apply the model to two different comets for which this ratio has already been measured with CN emission lines: C/2001 Q4 (NEAT) and C/2002 T7 (LINEAR).

In the next section the observational data are described for the two targets. Section 3 presents the models for the $^{12}C_2$ and $^{12}C^{13}C$ emission spectrum and Sect. 4 aims at comparing this model with the observations.

## 2. Observational data

Comet C/2001 Q4 (NEAT) was discovered on 24 August 2001 at 10 AU inbound surrounded by an 8-arcsec-wide coma, using

⋆ Based on observations made with ESO Telescopes at the Paranal Observatory under programmes ID 073.C-0525.

the 1.2-m Schmidt telescope on Palomar Mountain in the course of the Near-Earth Asteroid Tracking project NEAT of NASA's Jet Propulsion Laboratory (Pravdo et al. 2001). Orbital elements suggest that this object may come from the Oort Cloud, possibly on one of its first visits to the inner solar system. It was a bright comet with a total visual magnitude of ~2.8 as observed by ground-based observers when it passed closest to Earth on 6 May 2004. At that time the coma diameter was estimated to be 20 to 30 arcmin by amateur astronomers.

Comet C/2002 T7 (LINEAR) was discovered on 14 October 2002 at 6.9 AU inbound by the LINEAR project (Birtwhistle & Spahr 2002). It has a hyperbolic orbit, passed perihelion on 23 April 2004, and was 0.27 AU away from Earth on 19 May 2004. It was also a bright comet with an overall visual magnitude estimated at ~2.5 in May 2004.

Observations of comets C/2001 Q4 (NEAT) and C/2002 T7 (LINEAR) were carried out with the Ultraviolet-Visual Echelle Spectrograph (UVES) mounted on the 8.2-m UT2 telescope of the Very Large Telescope (ESO VLT). The two comets were observed on May 6 and 7 in visitor mode. They were both naked-eye objets in the evening and morning sky. Unfortunately, a strong earthquake in the morning of May 7 did not allow us to obtain another spectrum of T7 (LINEAR) in the $C_2$ setting. This comet was also observed later in service mode. UVES is a cross-dispersed echelle spectrograph designed to operate with high efficiency from the atmospheric cut-off at 300 nm to the long wavelength limit of the CCD detectors (about 1100 nm). Our spectra were obtained with a resolving power $\lambda/\Delta\lambda \sim 70\,000$. After data reduction (flat-fielding, wavelength calibration, background subtraction, proper order merging, cosmic ray removal, Doppler correction for geocentric velocity) we subtracted a solar spectrum convolved with the instrument response function (see Manfroid et al. 2009, for a more complete description of the data processing).

Table 1 presents the observing circumstances. The spectra were obtained in the inner part of the coma either on the nucleus or with a small offset to avoid as much of the strong solar continuum caused by dust scattering as possible. These offsets correspond to a maximum of ~3000 km of projected cometocentric distance.

## 3. Model for the $^{12}C_2$ and $^{12}C^{13}C$ emission spectrum

### 3.1. Modeling the $^{12}C_2$ spectrum

The $^{12}C_2$ radical is at the origin of many bright emission lines in the optical part of cometary spectra, the Swan bands. These bands were the first emission features detected in comets in the long-period comet Tempel 1864 II (Donati 1864). Because of the importance of the $^{12}C_2$ emission lines in comets, different works have been published for modeling the $^{12}C_2$ emission spectrum (Rousselot et al. 1994, 2000; Lambert et al. 1990; Gredel et al. 1989; Krishna Swamy & O'dell 1987; Lambert & Danks 1983). This is a difficult task for different reasons: (i) because of its homonuclear nature, this molecule has no permanent electric dipole moment, therefore electric dipole transitions among rotational and vibrational levels within an electronic state are forbidden (quadrupole transitions are negligible Arpigny 1965; pure vibration transitions through magnetic dipole radiation are forbidden Arpigny 1966); (ii) as a consequence, many levels corresponding to high rotational quantum numbers are populated and no serious fluorescence modeling can be performed without considering several thousand different levels; (iii) these radicals need a long time (several thousand seconds, i.e., several thousand kilometers of travel through the coma) to reach their fluorescence equilibrium; (iv) the main processes for de-exciting these radicals are intercombination transitions between $a^3\Pi_u$ and $X^1\Sigma_g^+$ states for which transition probabilities are poorly known.

The fluorescence equilibrium was completely treated (Rousselot et al. 2000) by considering six different electronic levels, each of them with its six first vibrational levels (from $v = 0$ to $v = 5$), each of them with all levels having a rotational quantum number $N \leq 90$. The total number of levels considered was 5652.

In a first step we improved and used this model for interpreting the $^{12}C_2$ observational spectra. Because our high-resolution spectra were obtained close to the nucleus (i.e., with $^{12}C_2$ molecules far from their fluorescence equilibrium), the result was imperfect. Our modeling was unable to correctly explain the intensity ratio of lines coming from levels with large differences in rotational quantum numbers. The intensities of the emission lines with low $N$ values were systematically underestimated. This was indeed expected, and such an effect had already been noticed by Lambert et al. (1990). These authors had noticed that, based on their fluorecence modeling, some low-$J'$ levels ($J' \leq 15$) appeared underpopulated in their spectra of comet 1P/Halley in the (0, 0) band. The plot of the relative populations (their Fig. 4) revealed that these can be fitted by two different rotational temperatures: a low one (665 K) for low-$J$ levels and a high one (3330 K) for high-$J$ levels.

Lambert et al. (1990) discussed the possible causes of this effect. After examining and rejecting different possible explanations (poor estimate of the intercombination transition moment $|R_e|^2$, possible role of the satellite transitions between $F_1$, $F_2$ and $F_3$ substates, collisions, etc.) they concluded that the low-T population originates in freshly formed $^{12}C_2$ molecules along the line of sight. The same authors suggested that the spectrum of these freshly formed $^{12}C_2$ molecules is also more sensitive to the influence of the satellite transitions. The influence of freshly formed $^{12}C_2$ molecules for the understanding of the observed spectrum was also confirmed, in a different way, by Rousselot et al. (1994), who noticed the long time needed by $^{12}C_2$ molecules to reach their fluorescence equilibrium.

Considering these previous works and the high resolution of our data, we chose to model the $^{12}C_2$ spectrum with a mixture of two different populations. The first possibility was to consider one population at fluorescence equilibrium and the other described by a Boltzmann distribution with a low temperature. The second option was to use two different Boltzmann distributions, one corresponding to a low temperature and another one corresponding to a high temperature. Because the final results for fitting the $^{12}C_2$ spectrum are rather similar (Rousselot et al. 2011), we preferred the second option, which had the advantage of easier calculations. Figure 1 presents the rotational structure of the two electronic states involved in the Swan bands as well as the transitions between these two states.

$^{12}C_2$ has electronic states with two different multiplicities (triplet and singlet states). Ground states for both multiplicities ($X^1\Sigma_g^+$ and $a^3\Pi_g$) are separated by only a few hundreds of cm$^{-1}$. Hence, some intercombination transition can arise between these two states. These singlet-triplet transitions are forbidden in electric dipole radiation, but can proceed by higher order multipole radiation. The corresponding transition probabilities are very low compared to other electronic transitions but they play a key role for understanding the fluorescence equilibrium by reducing the Boltzmann distribution of the level populations. The corresponding rotational temperature would be close to the color temperature of the Sun (i.e., $T \sim 5800$ K) without these transitions

**Table 1.** Observing circumstances.

| Comet | UT Date | $R$ | $\Delta$ | $V_r$ | $V_\Delta$ | Exp. time (s) | Offset |
|---|---|---|---|---|---|---|---|
| C/2002 T7 | 2004/05/06, 09:43 | 0.680 | 0.607 | 15.92 | –65.33 | 1080 | 5 |
| C/2002 T7 | 2004/05/25, 23:35 | 0.925 | 0.383 | 25.39 | 51.98 | 3208 | 0 |
| C/2001 Q4 | 2004/05/06, 01:34 | 0.977 | 0.321 | –5.36 | –3.31 | 2185 | 13 |
| C/2001 Q4 | 2004/05/07, 01:33 | 0.974 | 0.321 | –4.83 | –2.20 | 2144 | 13 |

**Notes.** $R$: Heliocentric distance (AU); $\Delta$: Geocentric distance (AU); $V_r$: Heliocentric velocity (km s$^{-1}$); $V_\Delta$: Geocentric velocity (km s$^{-1}$). The UT date corresponds to the beginning of the exposure. The offset of the slit with respect to the nucleus is given in arcsec.

**Table 2.** Hönl-London factors for the Swan transitions of $^{12}C_2$ (from Le Bourlot 1987).

| Transition | $P$ lines | $Q$ lines | $R$ lines |
|---|---|---|---|
| $^3\Pi_{g,0} \rightarrow {}^3\Pi_{u,0}$ | $J'+1$ | 0 | $J'$ |
| $^3\Pi_{g,1} \rightarrow {}^3\Pi_{u,1}$ | $J'(J'+2)/(J'+1)$ | $(2J'+1)/[J'(J'+1)]$ | $(J'+1)(J'-1)/J'$ |
| $^3\Pi_{g,2} \rightarrow {}^3\Pi_{u,2}$ | $(J'-1)(J'+3)/(J'+1)$ | $4(2J'+1)/[J'(J'+1)]$ | $(J'+2)(J'-2)/J'$ |

**Notes.** $J'$ is the upper rotational quantum number.

and is reduced to, typically, $T \sim 4000$ K for comets about 1 AU from the Sun.

Because $^{12}C_2$ is a homonuclear molecule with nuclear spin $I = 0$, all antisymmetric rotational levels are missing. For the $d^3\Pi_g$ and $a^3\Pi_u$ states these levels correspond to half the $\Lambda$-doublets, represented by dotted lines in Fig. 1. The three spin multiplet components are denoted $F_1$, $F_2$ and $F_3$, corresponding to the $^3\Pi_2$, $^3\Pi_1$ and $^3\Pi_0$ substates respectively (where the subscripts 2, 1, and 0 refer to the quantum number $\Omega$ that represents the total angular momentum of the electrons, including their spin).

Each rotational level is characterized by $N$, $J$ and $p$. $N$ is the angular momentum quantum number excluding electron spin. $J$ represents the total angular momentum quantum number excluding nuclear spin. $p$ is the parity (symmetric or antisymmetric level) that distinguishes the lambda substates. The parity is labeled with $e$ or $f$ (Brown et al. 1975) in Fig. 1, as well as with "+" and "−". In the $a^3\Pi_u$ electronic state all "+" levels correspond to antisymmetric levels and are, consequently, missing. The opposite situation holds in the $d^3\Pi_g$ state. The selection rules require that "+" rotational levels combine only with "−" rotational levels and "−" with "+" (Herzberg 1950). These rules correspond to $\Delta J = 0, e \leftrightarrow f$ and $\Delta J = \pm 1, e \leftrightarrow e$ and $f \leftrightarrow f$ (Brown et al. 1975).

Because our modeling is based only on two simple Boltzmann population distributions, there is no need to compute the fluorescence equilibrium with all electronic levels that can influence these populations, as performed by Rousselot et al. (2000), who chose the observational $^{12}C_2$ spectrum far from the nucleus to ensure that it would correspond to the fluorescence equilibrium.

Computing the $^{12}C_2$ emission spectrum implies knowledging of the energy levels and transition probabilities. For both states ($a^3\Pi_u$ and $d^3\Pi_g$) the energy levels were computed in a first step from the formulae and constants provided by Phillips (1968) with $T_v$ values from Tanabashi et al. (2007) (their Tables 3 and 4). We computed all energy values for the vibrational quantum number $v \leq 5$ and rotational quantum number $N \leq 100$. The corresponding line wavelengths provided by these constants and formulae were very accurate but, because of the high level of precision of our observational spectra (which implies an accuracy better than ~0.01 Å for the modeling), it was necessary to slightly improve the wavelengths in the region of interest. For this we used the High-Resolution Spectral Atlas of 122P/de Vico, which is available online (Cochran & Cochran 2002) in the region around the (2, 1) $^{12}C^{13}C$ bandhead.

The transition probabilities were computed following Rousselot et al. (2000). We used the Einstein $A_{v'v''}$ values published by Gredel et al. (1989) for the different bands and the Hönl-London factors given in Table 2.

The relative populations of the upper levels were computed in a two-step process. First the $x_i$ relative population of the different rotational levels belonging to the ground $a^3\Pi_u$ state were computed, using a Boltzmann distribution based on a rotational temperatures $T_{\rm rot}$ and a vibrational temperature $T_{\rm vib}$ according to the formula:

$$x_i = \frac{1}{Q}\exp\left(\frac{-1.439 \times E_v}{T_{\rm vib}}\right) \times \frac{1}{Q_v}(2J+1) \times \exp\left(\frac{-1.439 \times (E_{vJ\Omega} - E_v)}{T_{\rm rot}}\right).$$

In this formula $E_v$ is the vibrational energy (expressed in cm$^{-1}$), $E_{vJ\Omega}$ the energy of the vibrational and rotational level considered (also in cm$^{-1}$), $J$ the rotational quantum number of the rotational level considered, $Q$ the vibrational partition function and $Q_v$ the rotational partition function (for a given level $v$).

The partition functions, which normalized the sum of all the relative populations to 1, can be expressed as

$$Q = \sum_{v=0}^{5} \exp\left(\frac{-1.439 \times E_v}{T_{\rm vib}}\right)$$

and

$$Q_v = \sum_{N=1}^{100}\sum_{\Omega=0}^{2}(2J+1) \times \exp\left(\frac{-1.439 \times (E_{vJ\Omega} - E_v)}{T_{\rm rot}}\right).$$

Once the relative populations are known for the levels of the ground states, it is easy to compute those of the excited states, in the same way as in complete fluorescence equilibrium calculations (Rousselot et al. 2000). To compute the relative population

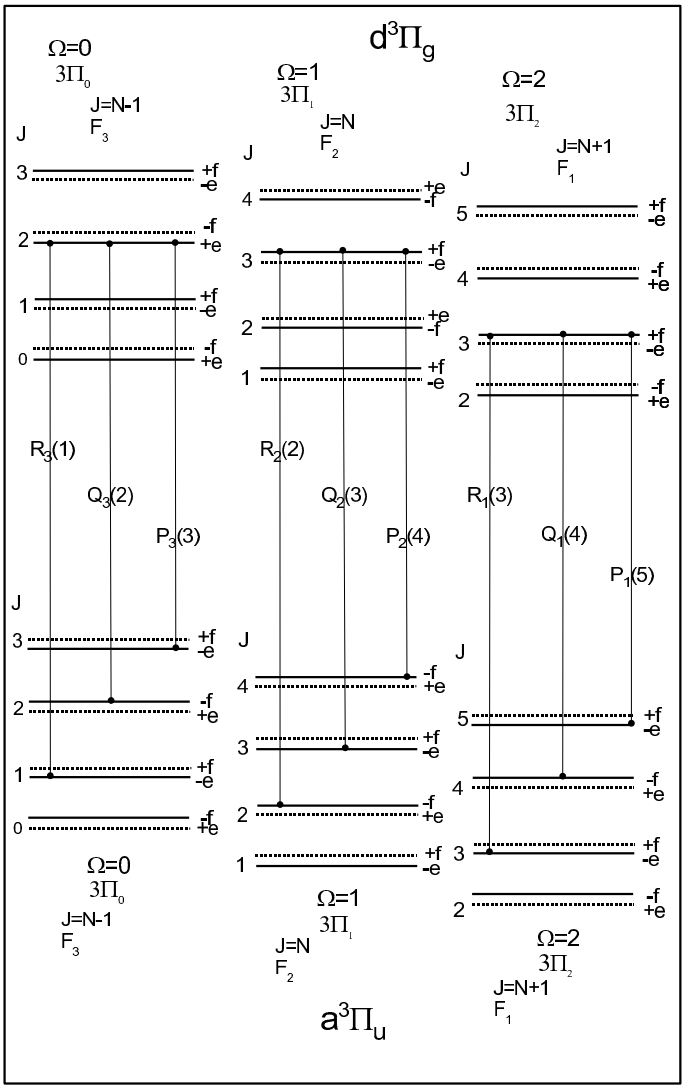


**Fig. 1.** Swan band transitions and structure of the rotational energy levels of $^{12}C_2$ for the $d^3\Pi_u$ and $a^3\Pi_g$ states. The dotted lines correspond to missing levels. The $Q_3$ lines have a zero transition probability, according to the Hönl-London factors given in Table 2. The $Q_2$ and $Q_1$ relative transition probabilities (compared to the $P$ and $R$ lines) rapidly decrease with increasing $J$ values.

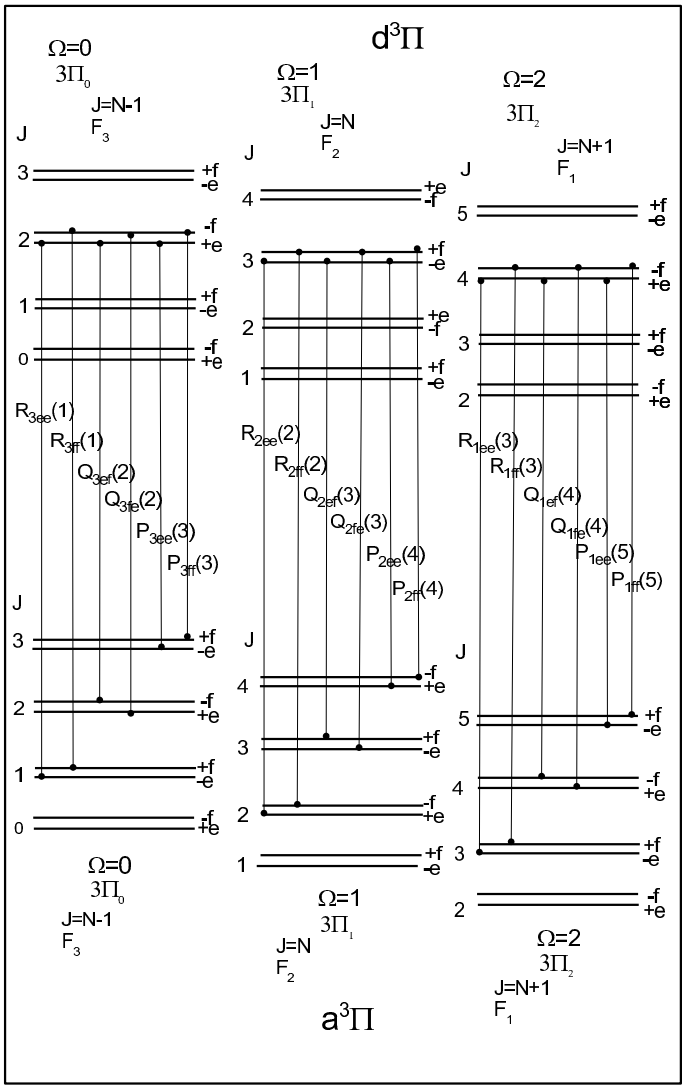


**Fig. 2.** Energy level diagram for the $^{12}C^{13}C$ Swan band transitions.

of a level $i$ belonging to the $d^3\Pi_g$ state we used the following relation:

$$\sum_{j=1}^{N_x} B_{ji}\rho_\nu x_j = \sum_{j=1}^{N_x} A_{ij}x_i,$$

where $\rho_\nu$ is the solar radiation density for the considered transition, $A_{ij}$ the Einstein coefficient for spontaneous emission and $B_{ji}$ the Einstein coefficient for absorption. In this equation $i$ denotes the upper level and $j$ the lower level with $N_x$ being the total number of lower rotational levels ($a^3\Pi_u$ state). This equation directly gives the $x_i$ values for the $d^3\Pi_g$ state sublevels:

$$x_i = \frac{\sum_{j=1}^{N_X} B_{ji}\rho_\nu x_j}{\sum_{j=1}^{N_X} A_{ij}}.$$

We used the high-resolution solar spectrum published by Kurucz et al. (1984) to compute the solar radiation density, in units of erg cm$^{-3}$ Hz$^{-1}$. The relative populations of the upper state led to the synthetic spectrum by using the line transition probabilities $A_{v'J'v''J''}$.

A good modeling of the observed $^{12}C_2$ emission spectrum required a mixing between two different synthetic spectra based on two different rotational temperatures. The unknown parameters to be determined are the two rotational temperatures (low and high) $T_{\mathrm{low_{rot}}}$ and $T_{\mathrm{high_{rot}}}$, the relative fraction of molecules corresponding to $T_{\mathrm{low_{rot}}}$ and the vibrational temperature $T_{\mathrm{vib}}$.

Because the latter parameter had little influence on our modeling it was taken equal to the temperature measured by other authors, i.e., around 4500 K for a comet located at 1 AU from the Sun. The three other free parameters were determined interactively by testing different solutions. In most cases the fraction of molecules corresponding to a low rotational temperature was small (~10%).

### 3.2. Modeling the $^{12}C^{13}C$ spectrum

The structure of the $^{12}C^{13}C$ is very similar to that of $^{12}C_2$, except that the antisymmetric levels are not missing because of the heteronuclear nature of this radical, in contrast to $^{12}C_2$. Figure 2 presents the energy level diagram with the transitions for the Swan bands of $^{12}C^{13}C$. It can be compared to Fig. 1. Each line

is now doubled because both components of the Λ-doublets are present. These components are equally populated.

For both states ($a^3\Pi$ and $d^3\Pi$) the energy levels are the sum of the electronic energy $T_e$, the vibrational energy $G(v)$, and the rotational energy $F(J)$. The $F(J)$ values were computed from the formulae and constants provided by Phillips (1968) for the $^{12}C_2$ radical, in which the constants were adapted to $^{12}C^{13}C$ according to the formulae given by Herzberg (1950). The $T_e$ and $G(v)$ values were taken from Tanabashi et al. (2007) and were also adapted to $^{12}C^{13}C$ for $G(v)$. We write (Herzberg 1950)

$$G(v) = \omega'_e\left(v+\frac{1}{2}\right) - \omega_e x'_e\left(v+\frac{1}{2}\right)^2 + \omega_e y'_e\left(v+\frac{1}{2}\right)^3 + \omega_e z'_e\left(v+\frac{1}{2}\right)^4,$$

where the vibrational constants $\omega'_e$, $\omega_e x'_e$, $\omega_e y'_e$ and $\omega_e z'_e$ for $^{12}C^{13}C$ were computed from the constants $\omega_e$, $\omega_e x_e$, $\omega_e y_e$ and $\omega_e z_e$ for $^{12}C_2$ by using the following formulae:

$$\omega'_e = \rho\omega_e$$
$$\omega_e x'_e = \rho^2\omega_e x_e$$
$$\omega_e y'_e = \rho^3\omega_e y_e$$
$$\omega_e z'_e = \rho^4\omega_e z_e,$$

in which $\rho = \sqrt{\mu/\mu_i}$, where $\mu$ and $\mu_i$ are the reduced masses of $^{12}C_2$ and $^{12}C^{13}C$ respectively. We used $\rho = 0.98052$.

For $^{12}C^{13}C$ we computed all energy values corresponding to the vibrational quantum number $v \leq 5$ and rotational quantum number $N \leq 100$. The transition probabilities were taken to be equal to those of $^{12}C_2$.

Because its dipole moment is negligible (Krishna Swamy 1987), $^{12}C^{13}C$ can be treated as a homonuclear molecule, i.e., its pure vibrational and rotational transitions can be neglected. Since these transitions have very low probabilities, we assumed that $^{12}C_2$ and $^{12}C^{13}C$ have similar vibrational and rotational excitation temperatures. These temperatures, as well as the relative fraction of radicals with a low $T_{rot}$, were taken to be equal to those of $^{12}C_2$ (determined by comparison with the observational spectrum).

The relative populations of the $d^3\Pi$ state were computed from those of the $a^3\Pi$ state. The only difference with the equations given above for $^{12}C_2$ is in the expression of $Q_v$ because both lambda doublets are now defined:

$$Q_v = \sum_{N=1}^{100}\sum_{\Omega=0}^{2} 2\times(2J+1)\times\exp\left(\frac{-1.439\times(E_{vJ\Omega}-E_v)}{T_{rot}}\right).$$

### 3.3. Determination of the $^{12}C^{13}C$ ratio

From the $^{12}C_2$ and $^{12}C^{13}C$ synthetic emission spectra it is possible to fit the data for different $^{12}C/^{13}C$ isotopic ratios (which correspond to twice the $^{12}C_2/^{12}C^{13}C$ ratios). The $^{12}C^{13}C$ spectrum is bright enough to be detected above the noise level for the (2, 1) and (1, 0) bands, which are located near 4723 and 4745 Å respectively.

Figures 3 and 4 present the synthetic spectra of $^{12}C_2$ and $^{12}C^{13}C$. The illustrated portion of the spectra corresponds to the $\Delta v = +1$ band sequence. The bandhead with the longer wavelength corresponds to the (1, 0) band, followed by the (2, 1) and (3, 2) bands of decreasing wavelengths. As already pointed out, the (1, 0) $^{12}C^{13}C$ bandhead lies completely outside the $^{12}C_2$ emission lines (near 4745 Å). Unfortunately, it is strongly blended with bright $NH_2$ emission lines, which must be fitted as well as possible to correctly reproduce the observed intensities.

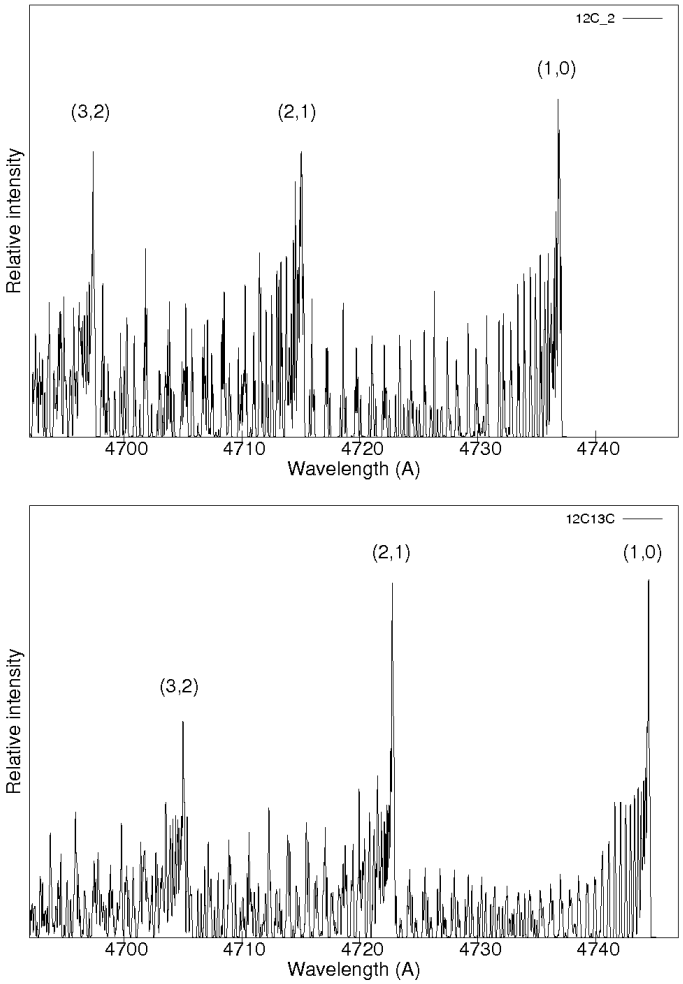


**Fig. 3.** Synthetic spectra of $^{12}C_2$ (*upper spectrum*) and $^{12}C^{13}C$ (*lower spectrum*) obtained using a mixture of two Boltzmann distributions with $T_{rot}$ = 4000 K and 600 K (90% and 10% of the molecules, respectively) and $T_{vib}$ = 4500 K. The emission lines were convolved with a Gaussian instrument response function of 0.07 Å FWHM, corresponding to the spectra provided by UVES.

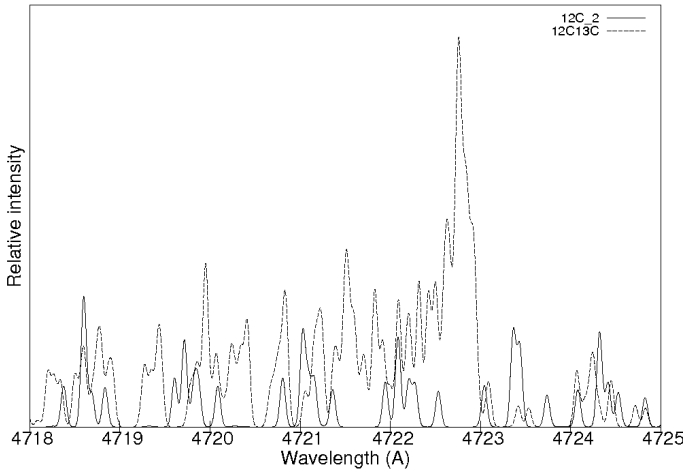


**Fig. 4.** Same spectra shown in Fig. 3 but represented together here at the same scale around the (2,1) bandhead of $^{12}C^{13}C$ near 4723 Å. Clearly this relatively bright bandhead is separated from the $^{12}C_2$ emission lines in these high-resolution spectra.

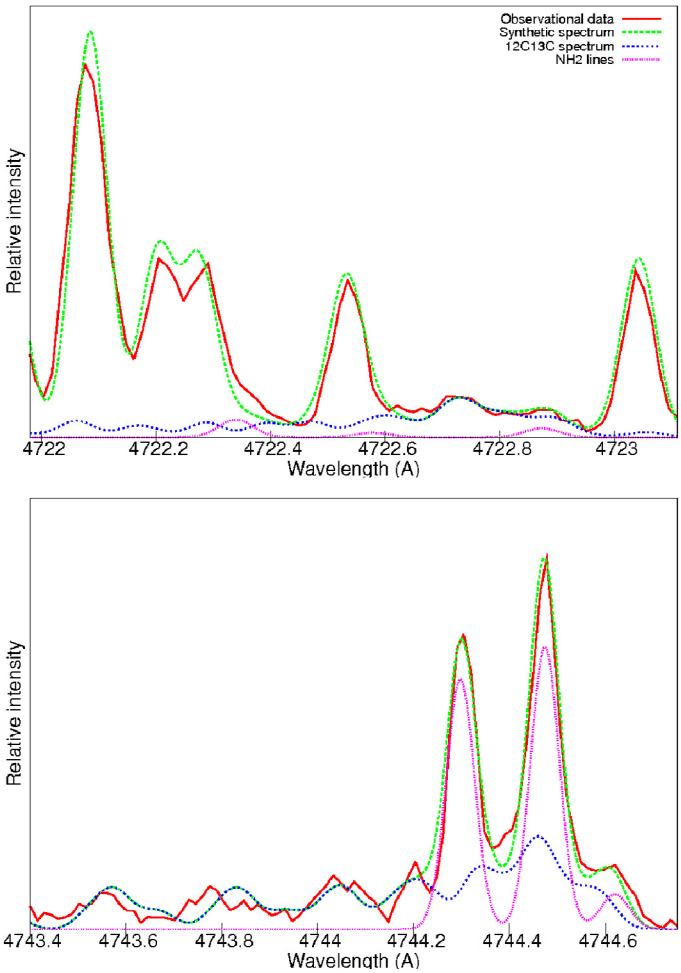


**Fig. 5.** Modeling of C/2001 Q4 (NEAT) spectrum obtained on 2004 May 7 with a mixture of two different Boltzmann distributions, respectively 4200 and 600 K with proportions of 90 and 10%. The *upper part* represents the region around the $(2,1)$ $^{12}C^{13}C$ band, the *lower part* the region around the $(1,0)$ $^{12}C^{13}C$ band. The importance of $(2,1)$ $^{12}C^{13}C$ and $NH_2$ lines is shown by their respective spectrum. The relative brightness of $NH_2$ lines have been adjusted to fit the observational data as well as possible.

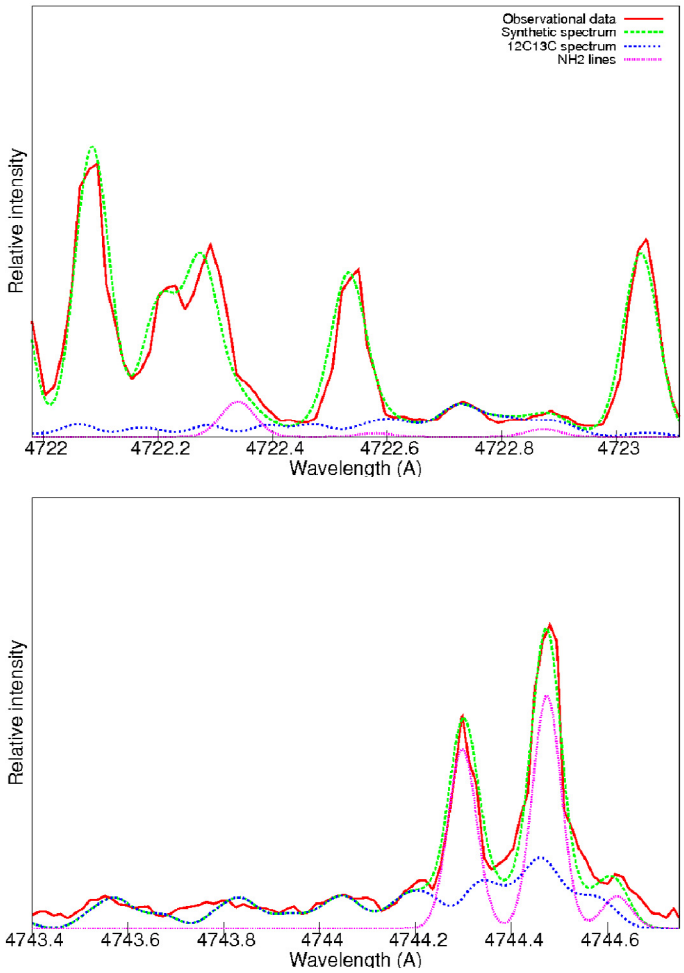


**Fig. 6.** Modeling of the C/2002 T7 (LINEAR) spectrum obtained on 2004 May 25 with a mixture of two different Boltzmann distributions, 3800 K and 600 K, with respective fractions of 80 and 20%. The *upper part* represents the region around the $(2,1)$ $^{12}C^{13}C$ band, the *lower part* the region around the $(1,0)$ $^{12}C^{13}C$ band.

## 4. Comparison with the observations

For each observational spectrum we first determined the best parameters by fitting the $^{12}C_2$ spectrum. These parameters are the two rotational temperatures, the relative population at those temperature, and the vibrational temperature. This vibrational temperature, which has little influence on the result, was chosen as a constant parameter with realistic values based on previous works dedicated to $^{12}C_2$ fluorescence modeling: 4800 K for the first spectrum (C/2002 T7 (LINEAR) with the shorter heliocentric distance) and 4500 K for the three others.

After a series of tests, good fits of the $^{12}C_2$ emission spectra were obtained. From the parameters used for the best fits we computed synthetic spectra of the $^{12}C^{13}C$ radical. For each observational spectrum, synthetic $^{12}C_2$ and $^{12}C^{13}C$ spectra were used with different $^{12}C/^{13}C$ ratios to fit the observational data as accurately as possible. The $^{12}C^{13}C$ wavelengths were slightly shifted to the blue for the (2, 1) band to adjust the bandhead to the observed spectrum. This small shift (about 0.03 Å) is within the uncertainty of the formulae used to compute the wavelengths.

**Table 3.** Comparison of our $^{12}C/^{13}C$ ratio determination with previous works, based on the CN B-X (0,0) emission band.

| Comet | This work | Previous work |
|---|---|---|
| C/2001 Q4 | 80 ± 20 | 70 ± 30 (Manfroid et al. 2005) |
| C/2002 T7 | 85 ± 20 | 85 ± 20 (Manfroid et al. 2009) |

Because of their strong influence, $NH_2$ emission lines were added to the final synthetic spectra with ad hoc intensities.

Figures 5 and 6 show the results obtained for both comets. The respective temperatures and fractions of molecules corresponding to the two rotational temperatures are given. These can be related to the offset and heliocentric distances given in Table 1. For C/2001 Q4 the main rotational temperature is higher than for C/2002 T7 (4200 K vs. 3800 K) and the proportion of molecules having this temperature (90% vs. 80%). This difference can be easily explained by the offsets, because the C/2002 T7 spectrum is obtained on the nucleus and the one of C/2001 Q4 at 13 arcsec (i.e., at about 3000 km of projected distance). In the second case the $C_2$ radicals have followed more absorption-emission cycles to reach their equilibrium temperature, corresponding to a higher rotational temperature.

**Table 4.** Previous measurements of the $^{12}C/^{13}C$ ratio based on the (1, 0) $^{12}C^{13}C$ bandhead.

| Comet | $^{12}C/^{13}C$ ratio | Author |
|---|---|---|
| Ikeya 1963 I | 70 ± 15 | Stawikowski & Greenstein (1964) |
| Tago-Sato-Kosaka 1969 IX | 100 ± 20 | Owen (1973) |
| Kohoutek 1973 XII | $115^{+30}_{-20}$ | Danks et al. (1974) |
| | $135^{+60}_{-45}$ | Danks et al. (1974) |
| Kobayashi-Berger-Milon 1975 IX | $100^{+20}_{-30}$ | Lambert & Danks (1983) |

We fitted the observational data by using an average $^{12}C/^{13}C$ ratio of 80 for C/2001 Q4 (NEAT) and 85 for C/2002 T7 (LINEAR) (80 for the first spectrum and 90 for the second). Nevertheless, the uncertainty on this measurement is significant and is estimated to be ±20. There is no significant difference according to the bandhead used. The uncertainty is due to the limit of our modeling, the weakness of the signal, and the difficulty to completely remove the solar continuum and the scattered light in UVES.

In Table 3 our determination of the $^{12}C/^{13}C$ ratio is compared to the one already published for the same comets, based on the CN B-X (0,0) emission band. Our results are consistent, within their uncertainty, with the results obtained from the modeling of the $^{12}CN$ and $^{13}CN$ B-X (0,0) bands.

## 5. Conclusion

The measurement of the $^{12}C/^{13}C$ ratio in comets is a challenge because the emission lines created by the radicals containing $^{13}C$ atoms (mainly CN or $C_2$) are weak. Using the (2, 1) $^{12}C^{13}C$ bandhead, in addition to the (1, 0), already used by other authors, is another way of measuring this ratio. It confirms previous results obtained either on the same comets with the $^{13}CN$ radical (cf. Table 3) or with the (1, 0) $^{12}C^{13}C$ bandhead observed in other comets (cf. Table 4).

Within the uncertainties, the $^{12}C/^{13}C$ ratios measured from two different species coming from different parent molecules are identical. This value also agrees with what is found in other primitive solar system objects. It thus seems that carbon did not suffer significant fractionation since the solar system formation.

Because of the weakness of these lines, which are located between brighter $^{12}C_2$ lines and are blended with $NH_2$ lines, and because of a critical subtraction of the solar continuum and the scattered light in the instrument, no significant improvement can be expected to reduce the uncertainty in determining the $^{12}C/^{13}C$ ratio. This method, nevertheless, yields errors similar to those obtained with CN spectra and proves to be a useful alternative or complementary technique.

*Acknowledgements.* J.M. is Research Director of the Belgian FNRS, E.J. is Research Associate of the Belgian FNRS and D.H. is Senior Research Associate of the Belgian FNRS.

## References

Arpigny, C. 1965, ARA&A, 3, 351
Arpigny, C. 1966, ApJ, 144, 424
Birtwhistle, P., & Spahr, T. B. 2002, IAU Circ., 8003, 1
Bockelée-Morvan, D., Biver, N., Jehin, E., et al. 2008, ApJ, 679, L49
Brown, J. M., Hougen, J. T., Huber, K.-P., et al. 1975, J. Mol. Spectrosc., 55, 500
Cochran, A. L., & Cochran, W. D. 2002, Icarus, 157, 297
Danks, A. C., Lambert, D. L., & Arpigny, C. 1974, ApJ, 194, 745
Donati, G. B. 1864, Astron. Nachr., 62, 375
Gredel, R., van Dishoeck, E. F., & Black, J. H. 1989, ApJ, 338, 1047
Herzberg, G. 1950, Molecular Spectra and Molecular Structure. I. Spectra of Diatomic Molecules, ed. Van Nostrand Reinhold company
Jehin, E., Manfroid, J., Hutsemékers, D., Arpigny, C., & Zucconi, J.-M. 2009, Earth Moon Planets, 105, 167
Jewitt, D., Matthews, H. E., Owen, T., & Meier, R. 1997, Science, 278, 90
Kleine, M., Wyckoff, S., Wehinger, P. A., & Peterson, B. A. 1995, ApJ, 439, 1021
Krishna Swamy, K. S. 1987, A&A, 187, 388
Krishna Swamy, K. S., & O'dell, C. R. 1987, ApJ, 317, 543
Kurucz, R. L., Furenlid, I., Brault, J., & Testerman, L. 1984, Solar flux atlas from 296 to 1300 nm
Lambert, D. L., & Danks, A. C. 1983, ApJ, 268, 428
Lambert, D. L., Sheffer, Y., Danks, A. C., Arpigny, C., & Magain, P. 1990, ApJ, 353, 640
Le Bourlot, J. 1987, Ph.D. Thesis, Université de Paris VII
Manfroid, J., Jehin, E., Hutsemékers, D., et al. 2005, A&A, 432, L5
Manfroid, J., Jehin, E., Hutsemékers, D., et al. 2009, A&A, 503, 613
McKeegan, K. D., Aléon, J., Bradley, J., et al. 2006, Science, 314, 1724
Owen, T. 1973, ApJ, 184, 33
Phillips, J. G. 1968, J. Mol. Spectrosc., 28, 233
Pravdo, S. H., Helin, E. F., Lawrence, K. J., et al. 2001, IAU Circ., 7695, 1
Rousselot, P., Clairemidi, J., & Moreels, G. 1994, A&A, 286, 645
Rousselot, P., Hill, S. M., Burger, M. H., et al. 2000, Icarus, 146, 263
Rousselot, P., Jehin, E., Manfroid, J., & Hutsemékers, D. 2011, in EPSC-DPS Joint Meeting 2011, held 2–7 October 2011 in Nantes, France, 602
Stadermann, F. J., Hoppe, P., Floss, C., et al. 2008, Meteorit. Planet. Sci., 43, 299
Stawikowski, A., & Greenstein, J. L. 1964, ApJ, 140, 1280
Tanabashi, A., Hirao, T., Amano, T., & Bernath, P. F. 2007, ApJS, 169, 472
Vanysek, V. 1977, in Comets, Asteroids, Meteorites: Interrelations, Evolution and Origins, ed. A. H. Delsemme, IAU Colloq., 39, 499
Wyckoff, S., & Wehinger, P. 1988, Chemical Abundance of Comets, Tech. rep.
Wyckoff, S., Lindholm, E., Wehinger, P. A., et al. 1989, ApJ, 339, 488
Wyckoff, S., Kleine, M., Peterson, B. A., Wehinger, P. A., & Ziurys, L. M. 2000, ApJ, 535, 991
Ziurys, L. M., Savage, C., Brewster, M. A., et al. 1999, ApJ, 527, L67